

## Article

# Microfabrication of VO<sub>2</sub> Thin Films via a Photosensitive Sol-Gel Method

Chuanbao Wu <sup>1,2,\*</sup>, Yunwei Wang <sup>3</sup> and Guangqiang Ma <sup>3</sup>

<sup>1</sup> College of Vanadium and Titanium, Panzhihua University, Panzhihua 617000, China

<sup>2</sup> Vanadium and Titanium Resource Comprehensive Utilization Key Laboratory of Sichuan Province, Panzhihua University, Panzhihua 617000, China

<sup>3</sup> School of Biological and Chemical Engineering, Panzhihua University, Panzhihua 617000, China; pzhuwyw001@163.com (Y.W.); magq3218@sina.com.cn (G.M.)

\* Correspondence: wuchuanbao@pzhue.edu.cn

**Abstract:** VO<sub>2</sub> films are widely used in photoelectric switches, smart glasses, storage media, and terahertz communications. In these applications, microfabrication technology is a very important process for producing microdevices or even improving film properties. In this paper, a novel photoetching microfabrication method is proposed for VO<sub>2</sub> thin films. First, a VO<sub>2</sub> precursor sol with ultraviolet photosensitivity was prepared using vanadyl acetylacetonate as the raw material and anhydrous methanol as the solvent. The dip-coated VO<sub>2</sub> gel film can be directly subjected to photolithography processing without coating additional photoresist by using the photosensitive sol. A fine pattern on the VO<sub>2</sub> film with good phase-transition performance can be obtained after annealing in a nitrogen atmosphere at 550 °C for 1 h. This method can be used to prepare grating, microarray, and various other fine patterns with the remarkable advantages of a low cost and simplified process, and the as-obtained material performances are unaffected using the method. It is a potential alternative method for optics, electronics, and magnetics devices based on VO<sub>2</sub> thin films.

**Keywords:** vanadium dioxide; photoetching; micro patterns; sol-gel method; phase transition



**Citation:** Wu, C.; Wang, Y.; Ma, G. Microfabrication of VO<sub>2</sub> Thin Films via a Photosensitive Sol-Gel Method. *Coatings* **2021**, *11*, 1264. <https://doi.org/10.3390/coatings11101264>

Academic Editor: Alexandru Enesca

Received: 23 August 2021

Accepted: 14 October 2021

Published: 18 October 2021

**Publisher's Note:** MDPI stays neutral with regard to jurisdictional claims in published maps and institutional affiliations.



**Copyright:** © 2021 by the authors. Licensee MDPI, Basel, Switzerland. This article is an open access article distributed under the terms and conditions of the Creative Commons Attribution (CC BY) license (<https://creativecommons.org/licenses/by/4.0/>).

## 1. Introduction

Vanadium dioxide (VO<sub>2</sub>) undergoes a metal-insulating phase transition (MIT) under thermal excitation at 68 °C, and its crystal structure will change from a low-temperature monoclinic M1 phase to a high-temperature rutile tetragonal phase [1–3]. The MIT process is accompanied by reversible saltation in optical, electrical, and magnetic properties [4–6]. Although the MIT behavior is observed in other transition-metal oxides, the phase-transition temperature of VO<sub>2</sub> is the closest to room temperature, and the phase transition is fast and reversible [7,8]. The unique properties of VO<sub>2</sub> near room temperature provide broad applications in the fields of photoelectric switches, smart glasses, storage media, and terahertz communications [9–12].

With the development of integration and miniaturization of micro-optoelectronic devices, microfabrication technology has gradually become more and more important, typically in the field of data storage and photoelectric switches [13,14]. In addition, one of the most promising applications of VO<sub>2</sub> is smart glasses, and a large number of studies on it have been reported. However, the low visible-light transmittance for coated VO<sub>2</sub> glass is one of the key issues [15–17], limiting its development. Recently, it has been reported that the preparation of moth-eye micro-nano structure patterns on the surface of VO<sub>2</sub> film can significantly improve its transmittance and also increase its infrared modulation ability [18]. In that study, the preparation method of its fine structure involves expensive equipment, and the process is complex, not suitable for large-scale production. Furthermore, the terahertz application of VO<sub>2</sub> has gradually become a new focus recently [19–21], and a low-cost and short-term microfabrication technology is urgently needed to prepare antenna patterns for terahertz communications.

In this study, a novel photoetching microfabrication method was developed to prepare micropatterns on VO<sub>2</sub> thin films via a photosensitive sol-gel process based on our previous study [22]. The process does not require photoresist, and it also does not require expensive ion etching equipment to instantly produce micron-level fine patterns. Moreover, the thin film micropattern process precedes the film annealing, which can avoid probable damage to the film performances observed in traditional microprocessing technologies. In particular, in our previous study, it is necessary to add a chelating agent or stabilizer to provide the sol photosensitive characteristic. In this study, a photosensitive VO<sub>2</sub> sol can be obtained only using the vanadyl acetylacetonate as the vanadium source and absolute methanol as the solvent without adding additional chelating agents or stabilizer. Owing to the simplification of composition of VO<sub>2</sub> sol, the pattern preparation process can be more easily controlled, and thus the VO<sub>2</sub> patterns of grating and microarray structures can be easily prepared.

## 2. Experiments

### 2.1. Preparation of VO<sub>2</sub> Micropatterns

A photosensitive VO<sub>2</sub> sol was prepared using vanadyl acetylacetonate as the raw material and anhydrous methanol as the solvent. The concentration of VO<sub>2</sub> sol was fixed at 0.1 mol/L by adjusting the amount of anhydrous methanol. The VO<sub>2</sub> sol was standing for 24 h at room temperature for aging. A VO<sub>2</sub> gel film was obtained on single-crystal silicon (100) or quartz substrates (only for UV-vis spectra test) by dip-coating with a withdrawal rate of 2 mm/s on a dip coater (DC-II, Xi'an University of Technology, Xi'an, China). Then, UV lithography was directly performed on the photosensitive gel film, as shown in Figure 1. A UV point light source (152 mW/cm<sup>2</sup>, SP-9, Ushio, Tokyo, Japan) was used to irradiate the gel film at room temperature for different times. The spot size is about 59 mm in diameter when the distance between the light source and film is 100 mm. The sample dimension is about 20 mm × 10 mm. The mask was fabricated by depositing Cr film onto a quartz substrate (processed by Shaopu Co. LTD, Changsha, China), according to the self-designed patterns. The irradiated gel film was then immersed in a mixture of ethanol and *n*-butanol (3:1 in volume) for 10 s and then blow-dried using nitrogen to develop the pattern. Thus, a fine pattern consistent with the negative image of the mask was obtained. Finally, the patterned gel film was annealed in a nitrogen atmosphere at 550 °C for 1 h to obtain a patterned VO<sub>2</sub> ceramic film.

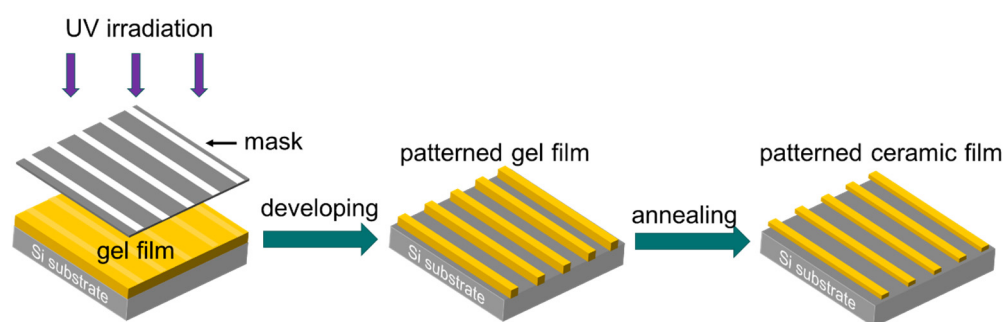


**Figure 1.** Schematic diagram of preparation process for patterned VO<sub>2</sub> ceramic film.

### 2.2. Characterization Techniques of VO<sub>2</sub> Micropatterns

The photodecomposition process of VO<sub>2</sub> gel film was studied by UV-Vis spectroscopy (D-7PC, Philes, Nanjing, China). The fine patterns of the film were observed by optical microscopy (DFC320, Leica Microsystems Ltd., Weztlar, Germany), an atomic force microscope (MFP-3D Infinity, Oxford Instruments, Oxford, England) and a scanning electron microscope (MCE, Tescan, Brno, Czech Republic). The phase structure of the film was tested using an X-ray diffractometer (X'Pert<sup>3</sup> Powder, PANalytical, Almelo, The Netherlands) in  $\theta$ -2 $\theta$  scan mode. The set voltage and current are 40 kV and 40 mA, respectively, the scanning angle is 20–60°, and the scanning step is 0.01°. To characterize the phase

transition of VO<sub>2</sub> film after microfabrication, the film was processed into a 50-micron-wide microbridge, and the resistance was tested using a four-lead method in the temperature range of 25–100 °C.

### 3. Results and Discussion

#### 3.1. Photosensitivity of VO<sub>2</sub> Gel Film

During the dissolution of vanadyl acetylacetonate in methanol, the carbonyl group of vanadyl acetylacetonate provides electrons to coordinate to the sixth vacant site of vanadium ions, forming a cyclic chelate [23]. The cyclic chelate can be maintained in the dip-coated VO<sub>2</sub> gel film, and it is gradually decomposed under UV-light irradiation to form an –O–V–O– network structure, which is insoluble in organic solvents, similar to the report in references [24,25]. On the other hand, the cyclic chelate still exists in the non-UV-irradiated gel film, and the gel film is easily dissolved in organic solvent. In this manner, the UV-irradiated VO<sub>2</sub> gel film will be retained, and the non-UV-irradiated gel film will be washed away after developing in organic solvents. Finally, a fine pattern consistent with the negative image of the mask can be obtained.

To study the photolysis kinetics process of VO<sub>2</sub> gel film under UV-light irradiation, a UV-vis spectrum test was carried out after UV exposure for every 20 min, and the time-gradient spectrum results are shown in Figure 2. A strong UV absorption peak for the VO<sub>2</sub> gel film appeared at about 302 nm, corresponding to  $\pi$ – $\pi^*$  transition in the cyclic chelate of vanadium [22]. The absorption intensity of cyclic chelate gradually decreased with increasing UV exposure time owing to the photodecomposition of cyclic chelate in the VO<sub>2</sub> gel film. Moreover, the rate of peak reduction gradually decreased. The peak intensity between the gel film irradiated for 60 min and irradiated for 80 min is similar, indicating that the cyclic chelate is nearly completely decomposed after UV irradiation for 60 min.

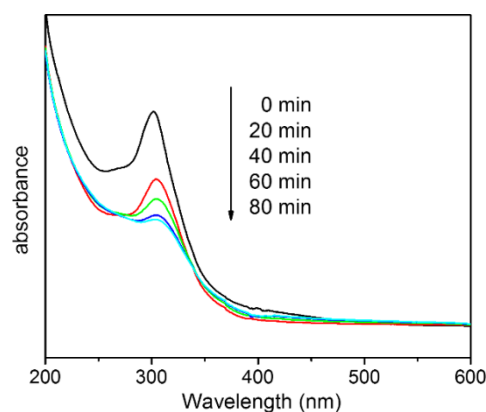


**Figure 2.** Time-gradient UV-vis spectra of VO<sub>2</sub> gel film coated on a quartz substrate.

#### 3.2. Patterns of VO<sub>2</sub> Films

In our experiments, it was found that, when a mixture of ethanol and *n*-butanol with a volume ratio of 3:1 was used to develop the UV-irradiated VO<sub>2</sub> gel film, a fine pattern with expected morphology can be obtained, as shown in Figure 3. In these patterns, the bright areas are the Si substrate, and the dark areas are the patterned VO<sub>2</sub> gel films apart from (i) and (j). Figure 3d shows that the film has a regular pattern and a uniform surface. The lithographic resolution can be evaluated to be about 5  $\mu$ m according to the radial-shape pattern in (c). Moreover, the microfabrication method can be used to produce both grating structures and dot array structures as shown in Figure 3e–j. It is believed that arbitrary micrographs with a size limit of more than 5  $\mu$ m can be obtained using the photosensitive sol-gel method as long as the mask patterns can be designed appropriately.

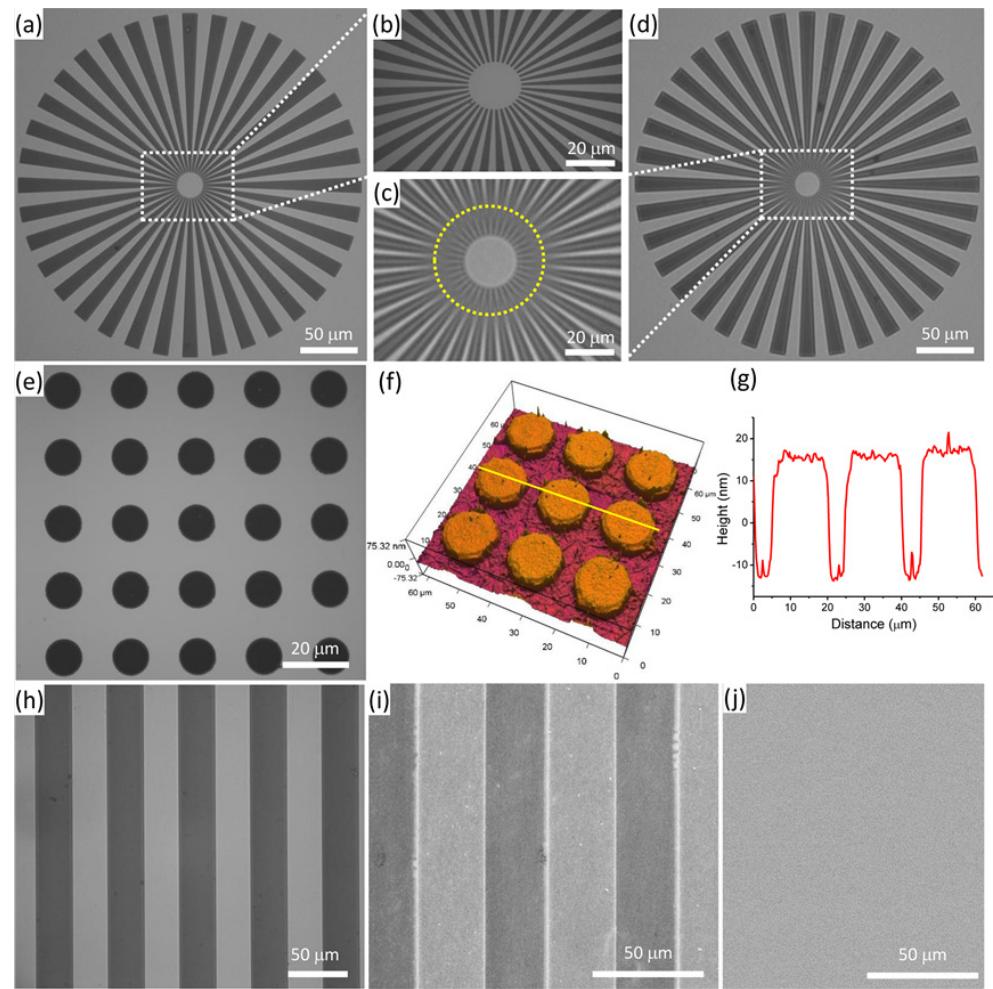


**Figure 3.** Mask plate of radial shape, patterned and also whole  $\text{VO}_2$  gel/ceramic films. (a) is a mask plate and (d) is the corresponding pattern on  $\text{VO}_2$  gel film. (b,c) is enlarged views of the boxed area in (a,d). The lines inside the circles in (c) can no longer be distinguished, so the lithographic resolution is evaluated to be  $5\ \mu\text{m}$ . (e–j) are patterned or whole  $\text{VO}_2$  ceramic films; (e) is a dot array with a periodicity of  $20\ \mu\text{m}$ , and (f,g) are the results from the atomic force microscope. (h) is grating with a periodicity of  $60\ \mu\text{m}$ ; (i,j) are scanning electron microscope pictures for grating patterns and whole films, respectively. There is almost no difference between the patterns and films.

### 3.3. Characteristics of $\text{VO}_2$ Ceramic Film

The  $\text{VO}_2$  film with a monoclinic M1 structure exhibits a remarkable phase-transition characteristic. To determine the phase structure of as-prepared film, a powder X-ray diffraction (XRD) experiment was performed on the  $\text{VO}_2$  film. Notably, the  $\text{VO}_2$  film was prepared by repeating the dip-coating and annealing processes for ten times to establish the film thickness (about  $310\ \text{nm}$ ) so as to enhance the XRD signals. Figure 4 shows the XRD pattern of  $\text{VO}_2$  ceramic film. Diffraction peaks are observed at angles of  $27.8^\circ$ ,  $37.0^\circ$ ,  $39.8^\circ$ ,  $55.5^\circ$ , and  $57.5^\circ$ , corresponding to the diffractive crystal planes of (011),  $(-211)$ , (020), (211), and (022) of  $\text{VO}_2$  material, consistent with the standard diffraction peaks of  $\text{VO}_2$  (JCPDS Card No. 82-0661) [26,27]. Notably, the peak intensity of (020) plane of obtained  $\text{VO}_2$  film is significantly higher than the corresponding intensity in the standard powder diffraction card. This indicates that the  $\text{VO}_2$  film has a certain (020) preferred orientation, which is derived from the single-crystal Si (100) substrate [28]. In addition, except for the diffraction peaks from  $\text{VO}_2$  film, no peaks were detected from the other impurities, demonstrating that a single-phase  $\text{VO}_2$  film with monoclinic M1 structure was obtained.

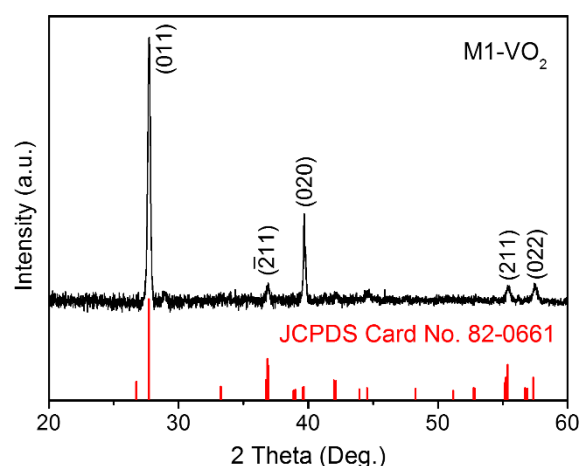


**Figure 4.** XRD pattern of VO<sub>2</sub> ceramic film grown on a single-crystal Si (100) substrate.

The phase-transition behavior of patterned VO<sub>2</sub> ceramic film was further investigated, and the resulting  $R$ - $T$  curve is shown in Figure 5. To eliminate the contact resistance, a four-lead method was used to test the resistance of patterned VO<sub>2</sub> ceramic film, as shown in the inset of Figure 5, which shows that, as the temperature increases, the resistance of patterned VO<sub>2</sub> film gradually decreases. The resistance then drops sharply at about 66 °C, indicating that the patterned film underwent a phase transition from a low-temperature insulating phase to a high-temperature metal phase at this temperature. The phase-transition process is completed at about 79 °C, and the resistance slowly decreases again as the temperature increases. During the cooling, a reversible phase transition occurs at about 63 °C, returning to the low-temperature insulating phase. During the entire phase transition, the saltation amplitude of resistance reaches about two orders of magnitude, similar to the phase transition of the VO<sub>2</sub> film reported in the literature [13,29]. It seems that the microfabrication method proposed in this study does not affect the phase-transition behavior of VO<sub>2</sub> film.

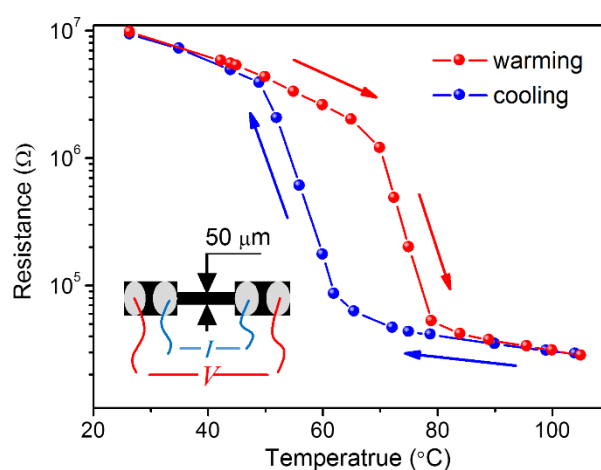


**Figure 5.**  $R$ - $T$  curve of patterned VO<sub>2</sub> ceramic film.

The microfabrication method proposed in this study can be used to prepare gratings, microarray structures, and other various micropatterns, and it can be widely used in micro devices such as photoelectric switches, storage media, and terahertz antenna. Although the resolution of patterns can achieve about 5 μm in this research, it is likely that the resolution can reach 1 μm by further improving the photosensitivity of VO<sub>2</sub> sol. In particular, if laser interferometry rather than UV irradiation is used for photolithography in the future, it will be able to achieve submicron resolution. In that case, the photosensitive sol-gel method might provide a new process route for improving the color of VO<sub>2</sub> film, increasing



the visible-light transmittance, and endowing superhydrophobic properties by designing applicable patterns [18].

#### 4. Conclusions

We developed a photosensitive sol-gel method to prepare micropatterns on VO<sub>2</sub> thin films. In this method, the UV-photosensitive VO<sub>2</sub> precursor sol was prepared using vanadyl acetylacetonate as the raw material. After UV-photoetching and developing in organic solvents, a VO<sub>2</sub> film micropattern consistent with the negative image of the mask was obtained. Finally, a remarkable phase-transition behavior was observed in the patterned VO<sub>2</sub> ceramic film after annealing in a nitrogen atmosphere at 550 °C for 1 h. The method does not require photoresist and expensive ion etching equipment, and the microfabrication process is simple. Furthermore, the obtained film has a regular pattern and uniform surface. In particular, the microfabrication process precedes the annealing process, so it does not affect the performances of the film. It is demonstrated that the microfabrication method proposed in this study can be used to prepare gratings and microarray structures. Therefore, the microfabrication process is a potential method for producing various photoelectric devices based on VO<sub>2</sub> film.

**Author Contributions:** C.W. conceived and conducted the experiments and wrote the preliminary version of the manuscript. Y.W. and G.M. discussed the results with C.W. and revised the paper. All authors have read and agreed to the published version of the manuscript.

**Funding:** This work was supported by the Sichuan Provincial Key Laboratory of Comprehensive Utilization of Vanadium and Titanium Resources (Grant No. 2018FTSZ30), the Science and Technology Project of Sichuan Province (Grant No. 2020ZHCG0098), and the Scientific Cultivation Project of Panzhihua University (Grant No. 2020ZD004).

**Institutional Review Board Statement:** Not applicable.

**Informed Consent Statement:** Not applicable.

**Data Availability Statement:** Not applicable.

**Conflicts of Interest:** The authors declare no conflict of interest.

#### References

1. Morin, F. Oxides which show a metal-to-insulator transition at the Neel temperature. *Phys. Rev. Lett.* **1959**, *3*, 34. [\[CrossRef\]](#)
2. Jones, A.C.; Berweger, S.; Wei, J.; Cobden, D.; Raschke, M.B. Nano-optical investigations of the metal-insulator phase behavior of individual VO<sub>2</sub> microcrystals. *Nano Lett.* **2010**, *10*, 1574–1581. [\[CrossRef\]](#)
3. Jeong, J.; Aetukuri, N.; Graf, T.; Schladt, T.D.; Samant, M.G.; Parkin, S.S.P. Suppression of metal-insulator transition in VO<sub>2</sub> by electric field-induced oxygen vacancy formation. *Science* **2013**, *339*, 1402. [\[CrossRef\]](#) [\[PubMed\]](#)
4. Li, W.W.; Yu, Q.; Liang, J.R.; Jiang, K.; Hu, Z.G.; Liu, J.; Chen, H.D.; Chu, J.H. Intrinsic evolutions of optical functions, band gap, and higher-energy electronic transitions in VO<sub>2</sub> film near the metal-insulator transition region. *Appl. Phys. Lett.* **2011**, *99*, 241903.
5. Stefanovich, G.; Pergament, A.; Stefanovich, D. Electrical switching and Mott transition in VO<sub>2</sub>. *J. Phys. Condens. Matter* **2000**, *12*, 8837. [\[CrossRef\]](#)
6. Liu, L.; Cao, F.; Yao, T.; Xu, Y.; Zhou, M.; Qu, B.; Pan, B.; Wu, C.; Wei, S.; Xie, Y. New-phase VO<sub>2</sub> micro/nanostructures: Investigation of phase transformation and magnetic property. *New J. Chem.* **2012**, *36*, 619–625. [\[CrossRef\]](#)
7. Kana Kana, J.B.; Vignaud, G.; Gibaud, A.; Maaza, M. Thermally driven sign switch of static dielectric constant of VO<sub>2</sub> thin film. *Opt. Mater.* **2016**, *54*, 165–169. [\[CrossRef\]](#)
8. Pellegrino, L.; Manca, N.; Kanki, T.; Tanaka, H.; Biasotti, M.; Bellingeri, E.; Siri, A.S.; Marré, D. Multistate memory devices based on free-standing VO<sub>2</sub>/TiO<sub>2</sub> microstructures driven by joule self-heating. *Adv. Mater.* **2012**, *24*, 2929–2934. [\[CrossRef\]](#) [\[PubMed\]](#)
9. Seyfour, M.M.; Binions, R. Sol-gel approaches to thermochromic vanadium dioxide coating for smart glazing application. *Sol. Energy Mater. Sol. Cells* **2017**, *159*, 52–65. [\[CrossRef\]](#)
10. Liu, K.; Lee, S.; Yang, S.; Delaire, O.; Wu, J. Recent progresses on physics and applications of vanadium dioxide. *Mater. Today* **2018**, *21*, 875–896. [\[CrossRef\]](#)
11. Gao, Y.; Luo, H.; Zhang, Z.; Kang, L.; Chen, Z.; Du, J.; Kanehira, M.; Cao, C. Nanoceramic VO<sub>2</sub> thermochromic smart glass: A review on progress in solution processing. *Nano Energy* **2012**, *1*, 221–246. [\[CrossRef\]](#)
12. Liu, M.; Hwang, H.Y.; Tao, H.; Strikwerda, A.C.; Fan, K.; Keiser, G.R.; Sternbach, A.J.; West, K.G.; Kittiwatanakul, S.; Lu, J.; et al. Terahertz-field-induced insulator-to-metal transition in vanadium dioxide metamaterial. *Nature* **2012**, *487*, 345–348. [\[CrossRef\]](#) [\[PubMed\]](#)

13. Dong, K.; Hong, S.; Deng, Y.; Ma, H.; Li, J.; Wang, X.; Yeo, J.; Wang, L.; Lou, S.; Tom, K.B.; et al. A Lithography-free and field-programmable photonic metacanvas. *Adv. Mater.* **2018**, *30*, 1703878. [[CrossRef](#)] [[PubMed](#)]
14. Koza, J.A.; He, Z.; Miller, A.S.; Switzer, J.A. Resistance switching in electrodeposited VO<sub>2</sub> thin films. *Chem. Mater.* **2011**, *23*, 4105–4108. [[CrossRef](#)]
15. Li, S.Y.; Niklasson, G.A.; Granqvist, C.G. Thermochromic fenestration with VO<sub>2</sub>-based materials: Three challenges and how they can be met. *Thin Solid Films* **2012**, *520*, 3823–3828. [[CrossRef](#)]
16. Wang, S.; Liu, M.; Kong, L.; Long, Y.; Jiang, X.; Yu, A. Recent progress in VO<sub>2</sub> smart coatings: Strategies to improve the thermochromic properties. *Prog. Mater. Sci.* **2016**, *81*, 1–54. [[CrossRef](#)]
17. Cao, X.; Chang, T.; Shao, Z.; Xu, F.; Luo, H.; Jin, P. Challenges and opportunities toward real application of VO<sub>2</sub>-based smart glazing. *Matter* **2020**, *2*, 862–881. [[CrossRef](#)]
18. Qian, X.; Wang, N.; Li, Y.; Zhang, J.; Xu, Z.; Long, Y. Bioinspired multifunctional vanadium dioxide: Improved thermochromism and hydrophobicity. *Langmuir* **2014**, *30*, 10766–10771. [[CrossRef](#)]
19. Schalch, J.S.; Chi, Y.; He, Y.; Tang, Y.; Zhao, X.; Zhang, X.; Wen, Q.; Averitt, R.D. Broadband electrically tunable VO<sub>2</sub> metamaterial terahertz switch with suppressed reflection. *Microw. Opt. Techn. Lett.* **2020**, *62*, 2782–2790. [[CrossRef](#)]
20. Zhang, Y.; Wu, P.; Zhou, Z.; Chen, X.; Yi, Z.; Zhu, J.; Zhang, T.; Jile, H. Study on temperature adjustable terahertz metamaterial absorber based on vanadium dioxide. *IEEE Access* **2020**, *8*, 85154–85161. [[CrossRef](#)]
21. Song, Z.; Zhang, J. Achieving broadband absorption and polarization conversion with a vanadium dioxide metasurface in the same terahertz frequencies. *Opt. Express* **2020**, *28*, 12487–12497. [[CrossRef](#)]
22. Wang, Y.; Zhao, G.; Wu, C.; Duan, Z. Preparation of micro-patterned CaMn<sub>7</sub>O<sub>12</sub> ceramic films via a photosensitive sol-gel method. *Coatings* **2019**, *9*, 650. [[CrossRef](#)]
23. Nagarajan, V.; Müller, B.; Storcheva, O.; Köhler, K.; Pöppel, A. Coordination of solvent molecules to VO(acac)<sub>2</sub> complexes in solution studied by hyperfine sublevel correlation spectroscopy and pulsed electron nuclear double resonance. *Res. Chem. Intermed.* **2007**, *33*, 705–724. [[CrossRef](#)]
24. Yan, F.; Zhao, G.; Song, N.; Zhao, N.; Chen, Y. In situ synthesis and characterization of fine-patterned La and Mn co-doped BiFeO<sub>3</sub> film. *J. Alloys Compd.* **2013**, *570*, 19–22. [[CrossRef](#)]
25. Yuanqing, C.; Fuxue, Y.; Gaoyang, Z.; Zhezhe, W. Photosensitive sol-gel preparation and direct micro-patterning of c-oriented ZnO film. *Appl. Surf. Sci.* **2011**, *257*, 6817–6820. [[CrossRef](#)]
26. Zhu, M.; Qi, H.; Li, C.; Wang, B.; Wang, H.; Guan, T.; Zhang, D. VO<sub>2</sub> thin films with low phase transition temperature grown on ZnO/glass by applying substrate DC bias at low temperature of 250 °C. *Appl. Surf. Sci.* **2018**, *453*, 23–30. [[CrossRef](#)]
27. Zhou, H.; Li, J.; Xin, Y.; Sun, G.; Bao, S.; Jin, P. Optical and electrical switching properties of VO<sub>2</sub> thin film on MgF<sub>2</sub> (111) substrate. *Ceram. Int.* **2016**, *42*, 7655–7663. [[CrossRef](#)]
28. Chae, B.-G.; Kim, H.-T.; Yun, S.-J.; Kim, B.-J.; Lee, Y.-W.; Youn, D.-H.; Kang, K.-Y. Highly oriented VO<sub>2</sub> thin films prepared by sol-gel deposition. *J. Solid State Electr.* **2005**, *9*, C12. [[CrossRef](#)]
29. Maaza, M.; Bouziane, K.; Maritz, J.; McLachlan, D.S.; Swanepool, R.; Frigerio, J.M.; Every, M. Direct production of thermochromic VO<sub>2</sub> thin film coatings by pulsed laser ablation. *Opt. Mater.* **2000**, *15*, 41–45. [[CrossRef](#)]